1-2017

Effects of JWH015 in cytokine secretion in primary human keratinocytes and fibroblasts and its suitability for topical/transdermal delivery

Alicia Bort

Perla A. Alvarado-Vazquez

Carolina Moracho-Vilrriales

Kristopher G. Virga

Giuseppe Gumina

See next page for additional authors

Authors
Alicia Bort, Perla A. Alvarado-Vazquez, Carolina Moracho-Vilrriales, Kristopher G. Virga, Giuseppe Gumina, Alfonso Romero-Sandoval, and Scott Asbill

Research Article

MOLECULAR PAIN

Molecular Pain
Volume 13: 1–16

DOI: 10.1177/1744806916688220
journals.sagepub.com/home/mpx
SAGE

Effects of JWH015 in cytokine secretion in primary human keratinocytes and fibroblasts and its suitability for topical/transdermal delivery

Alicia Bort[1,2,*], Perla A Alvarado-Vazquez[2,*], Carolina Moracho-Vilrriales[1], Kristopher G Virga[2], Giuseppe Gumina[2], Alfonso Romero-Sandoval[2] and Scott Asbill[2]

Abstract

Background: JWH015 is a cannabinoid (CB) receptor type 2 agonist that produces immunomodulatory effects. Since skin cells play a key role in inflammatory conditions and tissue repair, we investigated the ability of JWH015 to promote an anti-inflammatory and pro-wound healing phenotype in human primary skin cells.

Methods: Human primary keratinocytes and fibroblasts were stimulated with lipopolysaccharide. The mRNA expression of cannabinoid receptors was determined using RT-PCR. The effects of JWH015 (0.05, 0.1, 0.5, and 1 μM) in pro- and anti-inflammatory factors were tested in lipopolysaccharide-stimulated cells. A scratch assay, using a co-culture of keratinocytes and fibroblasts, was used to test the effects of JWH015 in wound healing. In addition, the topical and transdermal penetration of JWH015 was studied in Franz diffusion cells using porcine skin and LC-MS.

Results: The expression of CB1 and CB2 receptors (mRNA) and the production of pro- and anti-inflammatory factors enhanced in keratinocytes and fibroblasts following lipopolysaccharide stimulation. JWH015 reduced the concentration of major pro-inflammatory factors (IL-6 and MCP-1) and increased the concentration of a major anti-inflammatory factor (TGF-β) in lipopolysaccharide-stimulated cells. JWH015 induced a faster scratch gap closure. These JWH015'seffects were mainly modulated through both CB1 and CB2 receptors. Topically administered JWH015 was mostly retained in the skin and displayed a sustained and low level of transdermal permeation.

Conclusions: Our findings suggest that targeting keratinocytes and fibroblasts with cannabinoid drugs could represent a therapeutic strategy to resolve peripheral inflammation and promote tissue repair.

Keywords

Cannabinoid receptors, keratinocytes, fibroblasts, JWH015, cytokine

Date received: 16 September 2016; revised: 12 November 2016; accepted: 7 December 2016

Introduction

Tissue damage (i.e. surgeries, autoimmune conditions, chemotherapy, diabetes, herpes infections, etc.) triggers an inflammatory process that could result in chronic wounds, ulcers, irritation, pruritus, neuropathies or even sensitization of peripheral nociceptors, allodynia, and hyperalgesia.[1] Persistent peripheral inflammatory processes could subsequently induce changes in the central nervous system if they do not resolve in a timely fashion, as observed in major surgeries, rheumatoid arthritis, chemotherapy-induced neuropathy, diabetic peripheral neuropathy, and post-herpetic neuralgia. Therefore, a persistent peripheral inflammatory condition may result not only in chronic peripheral tissue damage but also in chronic pain.[2] Current available therapies for chronic

[1]Department of Biochemistry and Molecular Biology, School of Medicine, Alcalá de Henares, Madrid, Spain
[2]Department of Pharmaceutical and Administrative Sciences, Presbyterian College School of Pharmacy, Clinton, SC, USA

*Alicia Bort and Perla A Alvarado-Vazquez contributed equally to this article.

Corresponding author:
Alfonso Romero-Sandoval, Presbyterian College School of Pharmacy, 307 North Broad St, Clinton, SC, USA.
Email: asandoval@presby.edu

pain with prominent peripheral pathologic mechanisms act mostly in the central nervous system (antidepressants and anticonvulsants, cannabinoids, etc.), which not only induce many undesirable side effects but also provide partial relief only in a sub-population of patients.[3,4]

Pre-clinical models of inflammatory neuropathy have shown that targeting the peripheral source of inflammation (using clonidine) reduces pain-related behaviors in rats.[5–7] In clinical studies, the peripheral administration of clonidine reduces pain in patients with diabetic neuropathy.[8,9] Likewise, an 8% capsaicin patch is part of the current available arsenal to treat post-herpetic neuralgia.[10,11] These data provide a compelling argument in favor of peripherally directed therapies for the treatment of chronic pain with a predominant peripheral origin. The major advantage of these therapeutic strategies is the avoidance of central penetration to retain a desirable effect restricted to the periphery (i.e. topical drug administration and drugs that act on peripherally restricted targets), which will reduce central undesirable side effects (sedation, respiratory depression, paranoia, tolerance, etc.).

Due to the efficacy of cannabis in some types of chronic pain conditions,[12] synthetic cannabinoid molecules have been extensively studied in pre-clinical models with significant findings.[13,14] Even though cannabinoids could bind to different receptors (i.e. TRP channels, PPARs, GPR55, etc.), the effects of cannabis or other cannabinoids are mostly due to their actions on cannabinoid (CB) receptors type 1 (CB1), located mostly in the central nervous system, and CB receptors type 2 (CB2), located mostly in the periphery.[15,16] The major limitation of non-selective cannabinoids is their psychotropic side effects that depend upon central CB1 receptor activation.[17] Therefore, targeting peripheral CB1 receptors for the treatment of pain seems a safer pharmacological approach. Since CB2 receptors are predominantly expressed in the periphery (immune cells) and the central nervous system in non-neuronal cells (microglia), they represent attractive targets for the treatment of chronic pain. In fact, they are devoid of the classic cannabinoid psychotropic side effects (sedation, motor impairment, catalepsy, etc.) while possessing antinociceptive effects in rodent models even when administered intrathecally.[18,19] Based on preclinical models, the major mechanism of action of CB2 receptor agonists is the regulation of immune and inflammatory effectors to promote a homeostatic local milieu. Therefore, the use of selective CB2 agonists to target peripherally restricted cells would effectively modulate pro-nociceptive and pro-inflammatory effectors that could result in the treatment of local inflammation, promote tissue repair, and therefore prevent the development of chronic ulcers or chronic pain.

Immune cells have shown to be valid targets for the modulation of the local immune response in inflammatory conditions since they are the major sources of inflammatory products, and they express CB2 receptors. However, inflammation is a dynamic and complex process in which various types of immune cells act differently and at different times of the process.[20] This rather ever-changing inflammatory milieu could represent a challenge for the identification of the proper time window and the specific cell target to develop appropriate therapeutic approaches.

Peripheral cells, such as skin cells, not only have structural purposes but also play a critical role in the modulation of inflammation, tissue repair, and pain. For example, it has been demonstrated that keratinocytes are capable of evoking neuronal firing by the production of neuroactivators which could result in neuroinflammatory states or pain.[21] On the other hand, it has been shown that keratinocytes release β-endorphins via CB2 receptors, which results in the reduction of pain-related behaviors or endothelin-B receptor activation.[22] The external injection of a pro-algesic factor such as substance P into the rat hind paw induces an increase of nerve growth factor (NGF) in epidermal keratinocytes, which also increases the neuronal hyperexcitability.[23] Moreover, keratinocyte biopsies from human subjects with painful conditions such as complex regional pain syndrome type 1 (CRPS) or post-herpetic neuralgia showed a greater expression of sodium channels, which may contribute to the promotion and maintenance of pain.[24] Fibroblasts also play a role in pain, tissue repair, or inflammation. In rheumatoid arthritis, they promote leukocyte infiltration into the joints.[25] Moreover, an impairment in fibroblast growth can impair the proper wound closure.[26] Fibroblasts are also important in the transition from acute to chronic inflammation.[27,28] Due to the prominent role of keratinocytes and fibroblasts in inflammation, wound healing, and pain disorders, they are suitable targets as first responders of the inflammatory cascade following tissue damage. Since these skin cells express CB2 receptors,[29,30] they represent ideal targets for selective CB2 receptor agonists for inflammatory conditions.[31]

We hypothesize that the preferential activation of CB2 receptors will promote an anti-inflammatory phenotype in human primary keratinocytes and fibroblasts. To test our hypothesis, we first determined the suitability of keratinocytes and fibroblasts stimulated with lipopolysaccharide (LPS) to be treated with a CB2 receptor agonist by determining the expression of CB1 and CB2 receptors; second, we studied the immune capabilities of these cells by measuring production of pro- and anti-inflammatory effectors upon LPS stimulation; third, we studied the anti-inflammatory effects of JWH015 ((2-Methyl-1-propyl-1*H*-indol-3-yl)-1-naphthalenylmethanone), a preferential CB2 receptor agonist, in these cells by measuring its effects on the production of pro- and anti-inflammatory products; fourth, we tested

the CB2 receptor specificity of JWH015's effects by using AM630 or AM281 (selective CB2 and CB1 receptor antagonists/inverse agonists, respectively); fifth, we studied the potential effects of JWH015 in tissue repair by measuring wound healing capabilities of keratinocytes and fibroblasts using an in vitro scratch assay; and sixth, we determine the suitability of JWH015 to reach keratinocytes and fibroblasts when applied to the skin by measuring its topical and transdermal penetration in an ex vivo model.

Materials and methods

Cell culture

Human primary dermal fibroblasts (fibroblasts) were cultured in Dublecco's Modified Eagle Medium F12 medium (DMEM-F12, 1×) supplemented with 10% fetal bovine serum (FBS) and 1% penicillin/streptomycin (Gibco-Life Technologies, Grand Island, NY). Human primary epidermal keratinocytes (keratinocytes) were cultured in Dermal Cell Basal Medium supplemented with a keratinocyte growth kit that contained 0.4% (v/v) bovine pituitary extract, recombinant human tumor necrosis growth factor alpha (0.5 ng/mL), L-glutamine (6 mM), hydrocortisone hemisuccinate (100 ng/mL), recombinant human insulin (5 μg/mL), epinephrine (1 μM), and apo-transferrin (5 μg/mL) (Keratinocyte growth kit, ATCC, Manassas, VA). Keratinocytes or fibroblasts were generously gifted by Dr. Kim Creek (University of South Carolina, Columbia). These cells were obtained from human neonatal foreskin following circumcision from tissue that is routinely discarded with no protected health information linked to these samples and under the IRB protocol PHA IRB #2008-10 (Palmetto Health Institutional Review Board). Both cell types were plated in 75 cm^2 tissue flasks and incubated at 37°C in a 5% CO_2 atmosphere throughout the experiment. Media were changed every four to five days. We ceased use of cells after three passages. Cells were used when 100% confluence was reached. Cells were detached by adding 8 mL of trypsin/ethylenediaminetetraacetic acid (EDTA) to the flask for 5 min and incubated at 37°C in a 5% CO_2. The reaction was stopped with 500 μL of non-diluted FBS. Cells were counted and plated at the following concentrations: 100,000 cells/mL/well for keratinocytes when cultured alone and 100,000 cells/mL/well for fibroblasts when cultured alone. For scratch assays, cells were plated together in a co-culture containing 50,000 cells/mL of fibroblasts and 50,000 cells/mL of keratinocytes. Subsequently, the cells were incubated for 24 h in all cases before the addition of LPS stimulation and/or any pharmacological treatment. At this point, the media were changed and LPS was added with or without any pharmacological treatment, depending on the experimental paradigm. Each cell culture/experiment was performed using cells from one or two different independent donors. We performed the following experimental paradigms.

Experimental paradigm 1. This experiment was conducted to determine the time course of cytokine secretion by keratinocytes or fibroblasts after a challenge with LPS. Keratinocytes were stimulated with 10 μg/mL LPS, and fibroblasts were stimulated with 5 μg/mL LPS. LPS and its concentration were chosen, based on the literature and on our previous pilot experiments, in order to stimulate the cells.[32,33] LPS was dissolved in sterile distilled water (*Escherichia coli* O111:B4; Sigma Aldrich, St. Louis, MO). Supernatants were collected at 4, 24, 48, 72 and 96 h following the LPS challenge. Supernatants under these conditions were frozen at −80°C until cytokine assays.

Experimental paradigm 2. This experiment was conducted to determine the potency and efficacy of JWH015 in the production of pro- and/or anti-inflammatory factors by keratinocytes and fibroblasts. We constructed JWH015 dose–response curves using the following concentrations: 0.05, 0.1, 0.5 and 1 μM (dissolved JWH015 in 0.1% DMSO, to total 1 mL). JWH015 and LPS were added to the culture concomitantly (time 0). These studies were performed at a given time following LPS stimulation, and an incubation time point was chosen based on the first experimental design (24 h). Supernatants under these conditions were collected at the chosen time point and frozen at −80°C until pro- and anti-inflammatory products were measured.

Experimental paradigm 3. This experiment was conducted to determine whether JWH015's effects on pro- and/or anti-inflammatory products in keratinocytes or fibroblasts were exerted through CB1 and/or CB2 receptor activation. We aimed to block JWH015's effects with either the CB1 receptor antagonist/inverse agonist, AM281, or the CB2 receptor antagonist/inverse agonist, AM630 (dissolved in 0.2% DMSO, to total 1 mL for both AM218 and AM630). For either AM281 or AM630, a concentration of 1 μM was utilized, which is equivalent to the most effective concentration tested for JWH015. We have previously demonstrated that AM281 and AM630 at this concentration display an acceptable level of specificity for CB1 (AM281) and CB2 (AM630) receptors in in vitro cell cultures.[13] The antagonist/inverse agonist, LPS, and JWH015 were added to the culture concomitantly (time 0).

These studies were performed at a given time following LPS stimulation, and an incubation time point was chosen based on the first experimental design (24 h). We chose a given JWH015 concentration based

on the second experimental design (1 μM). Supernatants under these conditions were collected at the chosen time point and frozen at −80°C until pro- and anti-inflammatory products were measured.

Enzyme-linked immunosorbent sandwich assay analyses

The supernatant concentration of interleukin-6 (IL-6), monocyte chemoattractant protein-1 (MCP-1), transforming growth factor-beta (TGF-β), tumor necrosis factor-alpha (TNF-α), and IL-10 was measured with commercial enzyme-linked immunosorbent sandwich assay (ELISA) kits (human IL-6, human MCP-1, human TGF-β, human TNF-α, and human IL-10 ELISA Ready-SET-Go!; eBioscience, San Diego, CA). Sensitivity of the ELISA kits is as follows: 2 pg/mL for human IL-6 and IL-10, 8 pg/mL for MCP-1, and TGF-β, 4 pg/mL for TNF-α. These assays were performed following the manufacturer's instructions.

RNA isolation and quantitative RT-PCR

Cannabinoid receptor types 1 and 2 mRNA was determined 24 h following LPS stimulation in keratinocytes or fibroblasts. This time point was chosen based on the first experimental paradigm, described previously. Following cell incubation, the cells were washed with 1 mL of ice-cold sterile PBS, collected using BL + TG buffer (PBS and 1-thioglycerol), and stored at −80°C until RNA isolation experiments. RNA was isolated from both types of cells using Reliaprep RNA Cell Miniprep System (Promega, Madison, WI) according to manufacturer's protocols.

The levels of mRNA were determined as described previously.[34] Briefly, 1 μg of total RNA from each sample was reverse transcribed into cDNA using Script Reverse Transcription Supermix (BioRad, Hercules) in the following conditions: 5 min at 25°C, 30 min at 42°C, and 5 min at 85°C. We quantified the expression of CB1 (57°C), CB2 (57°C), and β-actin (57°C) using SsoAdvanced Universal SYBR Green Supermix (BioRad, Hercules, CA) in the following conditions: 1 cycle of 98°C for 30 s, 45 cycles of 98°C for 15 s, 30 s of the primer-specific annealing temperature. The primers for real-time (RT)-PCR are shown in the Supplementary Table 1. All samples were run in duplicate using the CFX96 Real-Time PCR system (Bio-rad, Hercules). A melt curve analysis was performed between 65°C and 95°C in 0.5° intervals (5 s per interval). The expression of mRNA for our molecules of interest was normalized to the β-actin expression level. Then, the fold change of the cannabinoid receptors was calculated using the values of non-stimulated cells (control), which was given a value equal to 1. The fold change of each gene was determined using the ddCt method, as previously described.[35]

Scratch assay

This in vitro assay is widely used to study some functional aspects of keratinocytes and fibroblasts in the wound healing process.[36–38] We conducted this experiment to determine whether the immunomodulatory effects of JWH015 on keratinocytes and fibroblasts affect their migration capabilities.

Keratinocytes and fibroblasts were cultured individually, as described previously, and co-cultured in Dermal Cell Basal Medium for 24 h at 37°C in 5% CO_2. The scratch was created in the cell monolayer using a 10 μL pipette tip. To make the scratch a consistent size, and to allow further imaging follow-up, two marks were made at the bottom of each well. The scratch was made between these marks in all cases. The cellular debris was removed (by replacing the media) then an LPS stimulus (10 μg/mL) and the pharmacological treatment were added when appropriate. The following groups were used: keratinocytes and fibroblasts stimulated with LPS in the presence or the absence of JWH015 (1 μM, 0.2% DMSO in PBS), keratinocytes and fibroblasts stimulated with LPS and JWH015 (1 μM, 0.2% DMSO in PBS) in the presence or in the absence of AM281 (CB1 receptor antagonist/inverse agonist, 1 μM, 0.2% DMSO in PBS) or AM630 (CB2 receptor antagonist/inverse agonist, 1 μM, 0.2% DMSO in PBS).

The migration capabilities of these cells to fill the scratch gap mimic a wound healing process.[36,37] This process was measured at base line (0 h), and at 4, 12, 17 and 24 h following the scratch. Six digital images (5×) per condition were taken at each time point in the same area, next to a line of reference that was drawn previously. Digital images were taken using a digital camera attached to a microscope (Leica Microscope Imaging Software, Leica Microsystems, Buffalo Grove, IL). These images were processed with SigmaScan Pro software (Systat Software Inc., San Jose, CA). For each picture, the remaining gap of the scratch was masked, and the number of pixels in that area was recorded. Thus, the scratch gap at time 0 produced a consistently higher number of pixels. The average value obtained for the six images was used to determine the gap value of each observation (six observations were made per group). The values obtained in each condition were normalized with their respective baseline values at time 0, to control for baseline variations.

Synthesis of compound JWH015

To test the pro- and anti-inflammatory effects of a CB2 agonist, we utilized a commercially available formulation

of JWH015 (Tocris Biosience, 155471-08-2, Ellisville, MO). Our purpose was to identify whether CB2 receptor agonists directly affect the functionality of keratinocytes and fibroblasts under inflammatory conditions. Therefore, a minimal transdermal penetration and/or a potential lipid depot effect formation were desirable. For our transdermal experiments, we synthesized JWH015 to provide the quantities that are needed for transdermal and topical testing.

The synthesis of JWH015 was performed in-house according to the combined, modified procedures of and Huffman and Dai[39] and Bell et al.[40] Briefly, 2-methylindole was *N*-propyl-substituted under strong, basic conditions using 1-bromopropane to afford the intermediate, 2-methyl-1-propylindole (Supplementary Figure 1). The reaction mixture was purified by TLC grade flash chromatography (1:19 ethyl acetate/hexanes) and the intermediate carried forward to the proceeding synthetic step. The compound 2-methyl-1-propylindole was converted to JWH015 through the addition of 1-naphthoyl chloride under the appropriate Friedel-Crafts acylation conditions. The reaction mixture was purified by TLC grade silica gel flash chromatography (1:24 ethyl acetate/toluene) and structurally characterized via ^{1}H nuclear magnetic resonance spectroscopy (NMR). The NMR signals were identical to the published values, and no impurities were detected. Elemental analysis of JWH015 met the American Chemical Society standards for purity (Anal. Calcd for $C_{23}H_{21}NO$: C, 84.37; H, 6.46; N, 4.28. Found: C, 84.25; H, 6.54; N, 4.23). The final product in the free base form was a clear to light straw colored viscous oil that appeared to demonstrate chemical instability upon exposure to light and/or air. Samples were stored in the dark at −20°C under nitrogen conditions following purification until the time of use.

Ex vivo JWH015 skin permeability studies

The transdermal absorption of JWH015 was studied utilizing porcine skin obtained from an abattoir (Thompson's Meat Market, Alexandria, AL). Modified Franz diffusion cells (diffusional area: 0.64 cm^2; receptor volume: 5.1 mL; Permegear Inc., Riegelsville, PA) were used as described previously.[41] The receptor chamber was filled with isotonic PBS at a pH of 7.4, maintained at 37°C ± 0.5°C, and continuously stirred at 600 r/min. Fresh porcine skin was secured in each of the diffusion cells and was allowed to equilibrate for 30 min, while bathed in PBS. Following equilibration, approximately 0.5 mL of the respective formulation was placed on each cell.

The samples of porcine skin were incubated with either 0.5 mL of mineral oil containing 5% JWH015 or 0.5 mL of the control vehicle containing mineral oil only. The samples (300 µL) were taken from the receptor chamber at 0.5, 1, 2, 3, 4, 5, 6, 12, and 24 h. The volume of each sample was immediately replaced with fresh PBS following sample collection, as described previously.[41] Samples were stored at −80°C until further analysis. The samples were analyzed using liquid chromatography-mass spectrometry (LC-MS). The drug concentration was measured and represented as µg/cm^2.[41]

Porcine skin extractions of JWH015

After the 24-h time point in the skin permeability studies, the porcine skin was collected to determine the amount of drug present in each of the skin samples. The mass of the porcine skin portion that was exposed to the formulation was resected, washed, and weight recorded. The skin was then dissected and diluted with dichloromethane at a ratio of 1 g:10 mL. An OmniTHQ Digital Tissue Homogenizer (Omni International, Kennesaw, GA) was used to homogenize each skin sample. After being mixed, 1 mL of supernatant was placed in an Eppendorf tube and centrifuged at 11,000 r/min for 30 min (Fisher Scientific AccuSpin Micro 17, Germany). The supernatant was collected and frozen at −80°C for further LC-MS analysis. The drug concentration was measured and represented as mg/g.[42]

LC-MS analysis of JWH015 for transdermal samples

All transdermal samples were spiked with 100 µL of an approximately 2.5 ppb solution of deuterium-labeled internal standard (JWH015-d7) obtained from Cayman Chemical Co (Ann Arbor, MI). Samples were then quantitatively transferred to LC autosampler vials and capped. Standards were prepared with concentrations ranging from 0.2 ppb to 10 ppb. Each standard solution was spiked with 100 µL of the deuterium-labeled internal standard, mentioned above.

The following are the parameters used for the LC analyses: Waters Acquity Classic binary pump; Column: Chromegabond WR C18 3 µm particles 15 cm × 2.1 mm (ES Industries, West Berlin, NJ); Gradient: Solvent A: Water with 0.1% formic acid; Solvent B: Acetonitrile with 0.1% formic acid; Flow rate: 200 µL/min. The time and composition used are as follows: 0 min, 25% B; 2 min, 25% B; 15 min, 100% B; 20 min, 100% B; 20.1 min, 25% B.

The following are the parameters used for the MS analyses: Waters Quattro Premier XE triple quadupole mass spectrometer; Ionization: positive ion electrospray. The desolvation gas flow was set to 700 L/h at a temperature of 350°C; the cone gas flow was set to 15 L/h. Collision gas was Ar set to 0.25 mL/min resulting in a cell pressure of 3.3×10^{-3} mbar. The mass spectrometer was operated in MRM mode, monitoring two transitions; one for the analyte 328 m/z > 155 m/z and one for the internal standard 335 m/z > 155 m/z. Each transition

had a 100 ms dwell time with a 50 ms interchannel delay and a 50 ms interscan delay. A cone voltage of 25 V was set for both transitions. A collision energy of 20 eV was used for both analyte and internal standard.

Levels of analyte in each sample were determined using the internal standard method. A calibration was generated by injecting three replicates of four standards. Linear regression with $1/\times$ weighting was used to produce the calibration curve.

LC-MS analysis of JWH015 for skin samples

All skin samples were blown down to dryness with a gentle stream of nitrogen and reconstituted in 3 mL of chloroform. Ten microliters of each sample were then transferred to LC sample vials containing 1.5 mL acetonitrile and 200 µL of a 3 ppm internal standard solution. Standards were prepared with concentrations ranging from 50 ppb to 1.3 ppm. Each standard was spiked with 200 µL internal standard as above.

Statistical analysis

All the statistical analyses were performed using GraphPad Prism 6.01 (GraphPad Software Inc., La Jolla, CA). Two-tailed unpaired t-tests and one- or two-way ANOVAs followed by Bonferroni's or Dunnett's post hoc were used as appropriate. A value of 0.05 was considered as statistically significant. Dose–response curves were obtained using a non-linear regression fitting method. The EC50 values were calculated using normalized-response-variable hill slope function to the data ($Y = 100/(1 + 10(\text{LogEC50-X}) \times \text{Hill Slope})$. The number of samples per group was based on the minimum number of data needed for statistical power (0.80) and significance (0.05), as determined from previous similar analyses.

Results

Cannabinoid receptors' mRNA in LPS-stimulated fibroblasts and keratinocytes

We determined the baseline expression of cannabinoid receptors mRNA in keratinocytes and fibroblasts at 24 h and after an LPS challenge. The LPS concentration we used to produce cell activation was based on the literature and on our previous pilot experiments.[32,33] We used 5 µg/mL of LPS to stimulate fibroblasts, and 10 µg/mL of LPS to stimulate keratinocytes. We observed that LPS stimulation produced a significant up-regulation of CB1 (Figure 1(a)) and CB2 (Figure 1(b)) mRNA in both keratinocytes and fibroblasts, when compared to non-stimulated cells.

Cytokine expression in keratinocytes and fibroblast after LPS challenge

We measured the cytokine concentration in cultures of either keratinocytes or fibroblast at different time points (4, 24, 48, 72 and 96 h) after an LPS challenge to determine the best time point to test the effects of JWH015.

When we stimulated keratinocytes with 10 µg/mL of LPS, we found a significant increase in IL-6 from 4 to 96 h after stimulation. The levels of IL-6 peaked at 48 h and remained at this level 72 and 96 h after LPS stimulation (Figure 2(a)). The levels of MCP-1 produced by LPS-stimulated keratinocytes significantly increased at 4 h and remained elevated until 96 h after LPS stimulation (Figure 2(b)). The concentration of TGF-β from

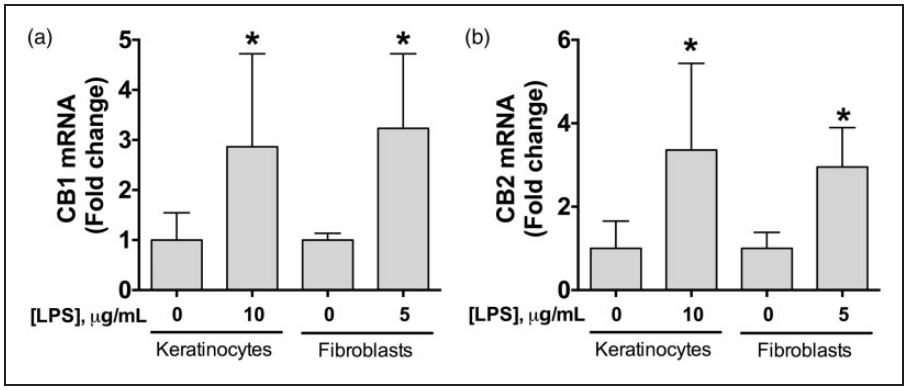

Figure 1. Expression of CB1 and CB2 receptors in human keratinocytes or fibroblasts following LPS stimulation. Quantification of CB1 (a) and CB2 (b) mRNA expression in LPS-stimulated keratinocytes or fibroblasts. The gene expression of CB1 or CB2 was normalized to the respective levels of β-actin in each sample and then calculated as fold change against the control group (non-stimulated cells), which was assigned a value equal to 1. Data shown are means ± SD; $n = 5$–6 samples. *$P < 0.05$ vs. non-stimulated cells using Student's t-test. LPS: lipopolysaccharide; CB1: cannabinoid receptor 1; CB2: cannabinoid receptor 2.

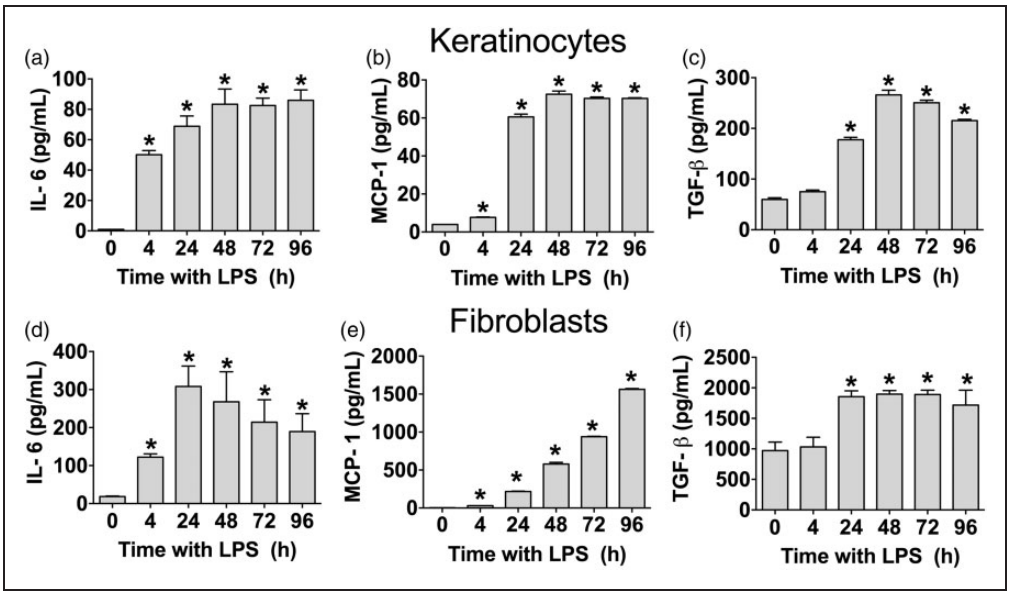

Figure 2. Effect of LPS in cytokine concentration in primary human fibroblast or keratinocyte cultures. Quantification of IL-6 (a and d), MCP-1 (b and e) and TGF-β (c and f) from supernatants of keratinocytes or fibroblasts (respectively) stimulated with LPS (10 and 5 μg/mL, respectively). Each bar represents the mean ± SD of 6 samples. *$P < 0.05$ vs. 0 h by using One-way ANOVA followed by Dunnett's post hoc test. LPS: lipopolysaccharide; IL-6: interleukin-6; MCP-1: monocyte chemoattractant protein-1; TGF-β: transforming growth factor-beta.

LPS-stimulated keratinocyte culture increased from 24 to 96 h after stimulation, peaking at 48 h (Figure 2(c)).

Fibroblasts that were stimulated with 5 μg/mL of LPS displayed an increase in IL-6 concentration from 4 h to 96 h. The maximum amount of IL-6 in fibroblasts was found at 24 h after LPS stimulation (Figure 2(d)). The levels of MCP-1 produced by LPS-stimulated fibroblast increased from 24 to 96 h and reached its highest concentration at 96 h after LPS stimulation (Figure 2(e)). The levels of TGF-β produced by LPS-stimulated fibroblasts significantly increased at 24 h and remained stable until 96 h after LPS stimulation (Figure 2(f)). We did not detect IL-10 or TNF-α in either keratinocytes or fibroblasts; the concentrations of these cytokines were below the sensitivity level of the ELISA kits used.

Based on these results, we tested the effects of JWH015 at 24 h after LPS stimulation in both keratinocytes and fibroblasts. We decided to test at 24 h of incubation because LPS consistently produced effects in all the detected cytokines at this time point.

The effects of JWH015 on LPS-stimulated keratinocytes and fibroblast

Keratinocytes and fibroblasts were stimulated with LPS and treated, concomitantly, with different concentrations of either JWH015 (0.05, 0.1, 0.5, and 1 μM) or its vehicle control (0.1% DMSO in saline) for 24 h. As previously reported, LPS induced an increase in IL-6, MCP-1, and TGF-β in both keratinocytes and fibroblast (Figure 3, gray bars).

When JWH015 was added to LPS-stimulated keratinocytes, we observed a significant decrease in IL-6 (Figure 3(a)). The percent effect curve of JWH015 for IL-6 concentration in keratinocytes is displayed in Figure 4(a).

When JWH015 was added to LPS-stimulated keratinocytes, we observed a significant decrease in MCP-1. This effect was concentration dependent (Figure 3(b)). The percent effect curve of JWH015 for MCP-1 concentration in keratinocytes is displayed in Figure 4(b).

Keratinocytes stimulated with LPS and, concomitantly, treated with JWH015 displayed elevated levels of TGF-β compared to the vehicle control group. This effect was concentration dependent (Figure 3(c)) and consistent with an anti-inflammatory effect. The percent effect curve of JWH015 for TGF-β concentration in keratinocytes is displayed in Figure 4(c). The minimum effective dose, efficacy, and potency of JWH015 for all these factors in keratinocytes are displayed in Table 1.

We determined that the addition of LPS alone ($87.95 \pm 1.8\%$ of viable cells) or LPS with JWH015 ($88.9 \pm 1.3\%$ of viable cells) did not produce any significant cytotoxicity in keratinocytes when compared to non-stimulated cells ($92.2 \pm 1.8\%$ of viable cells).

Fibroblasts stimulated with LPS and treated with JWH015 for 24 h exhibited a concentration-dependent decrease in IL-6 (Figure 3(d)). The percent effect curve of JWH015 for IL-6 concentration in keratinocytes is displayed in Figure 4(d).

When JWH015 was added to LPS-stimulated fibroblasts, we observed a significant, concentration-dependent

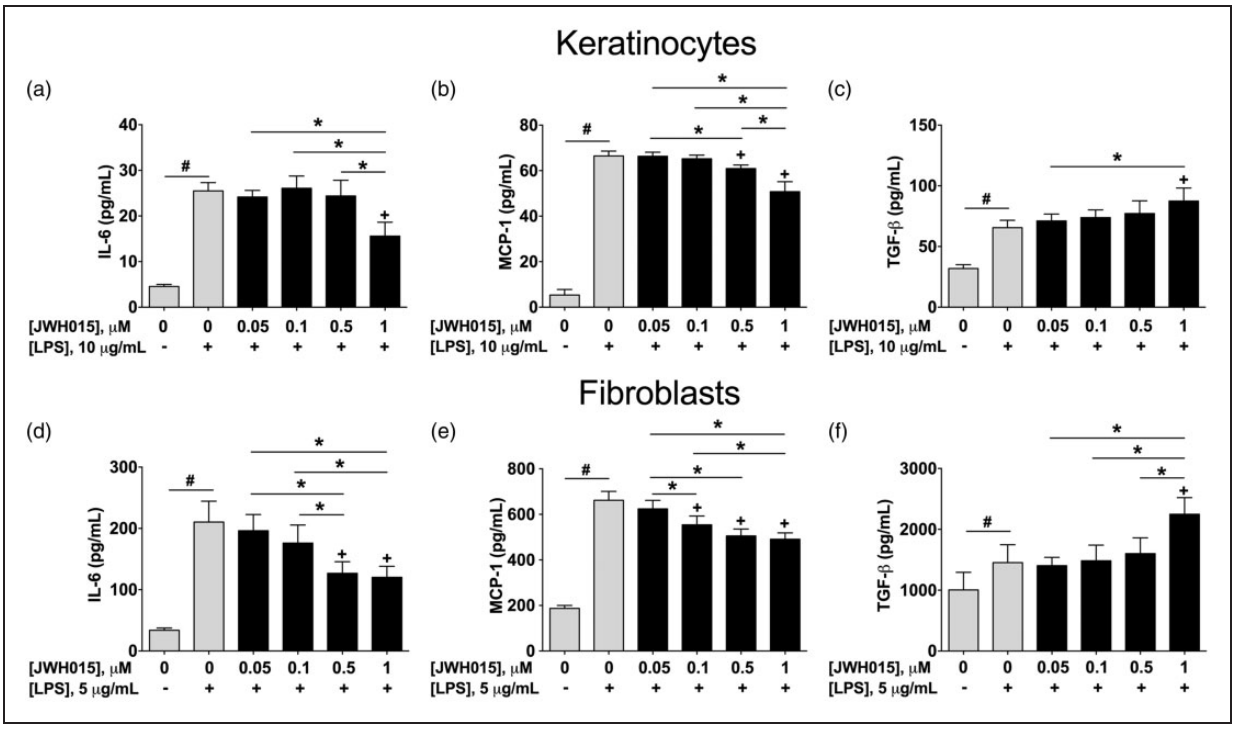

Figure 3. Effects of JWH015 in cytokines produced by keratinocytes or fibroblasts challenged with LPS. Quantification of IL-6 (a and d), MCP-1 (b and e) and TGF-β (c and f) in keratinocytes or fibroblasts (respectively) stimulated with LPS (10 and 5 μg/mL, respectively) for 24 h and treated with increasing concentrations of JWH015. Each bar represents the mean ± SD of 6 samples. $^{\#}P < 0.05$ vs. non-stimulated cells, $+P < 0.05$ vs. control group (LPS + vehicle) using One-way ANOVA followed by Dunnett's post hoc test. $^{*}P < 0.05$ between connected groups using One-way ANOVA followed by Tukey's post hoc test. Lipopolysaccharide; IL-6: interleukin-6; MCP-1: monocyte chemoattractant protein-1; TGF-β: transforming growth factor-beta.

decrease in MCP-1 (Figure 3(e)). The percent effect curve of JWH015 for MCP-1 concentration in keratinocytes is displayed in Figure 4(e).

Fibroblasts stimulated with LPS and, concomitantly, treated with 1 μM of JWH015 displayed an increase of TGF-β (Figure 3(f)). The percent effect curve of JWH015 for TGF-β concentration in keratinocytes is displayed in Figure 4(f). The minimum effective dose, efficacy, and potency of JWH015 for all these factors in fibroblasts are displayed in Table 1.

We determined that the addition of LPS alone (88.1 ± 2.1% of viable cells) or LPS with JWH015 (86.9 ± 5.5% of viable cells) did not produce any significant cytotoxicity in fibroblasts when compared to non-stimulated cells (92.3 ± 1.7% of viable cells).

Based on these results, we decided to use 1 μM of JWH015 to test the involvement of CB1 and CB2 receptors on the effects of JWH015.

Blockade of JWH015's effects using CB1 and CB2 antagonist/inverse agonists

Keratinocytes or fibroblasts were stimulated with LPS and concomitantly incubated with JWH015 (1 μM) alone, JWH015 (1 μM) + AM281 (1 μM), or JWH015 (1 μM) + AM630 (1 μM). Cytokine release was 24 h after the addition of the drugs, since JWH015 consistently produced an anti-inflammatory phenotype at this time point. As previously shown, we observed that the addition of LPS increased the concentration of IL-6, MCP-1, and TGF-β in both keratinocytes and fibroblasts incubated for 24 h (gray bars, Figure 5).

The concentration of IL-6 was significantly reduced by the addition of JWH015 to LPS-stimulated keratinocytes. This effect of JWH015 on IL-6 was completely blocked by AM630, and partially blocked by AM281 (CB2 and CB1 antagonist/inverse agonist, respectively; Figure 5(a)). Similarly, the concentration of MCP-1 was significantly decreased by JWH015 when added to LPS-stimulated keratinocytes, as described before. This decrease of MCP-1 induced by JWH015 was blocked by AM630 (CB2 antagonist/inverse agonist), but not by AM281 (CB1 antagonist/inverse agonist; Figure 5(b)). The addition of JWH015 to LPS-stimulated keratinocytes increased the concentration of TGF-β, as previously shown, and this effect was blocked by either AM630 or AM281 antagonists/inverse agonists (Figure 5(c)).

The concentration of IL-6 was significantly reduced by the addition of JWH015 to LPS-stimulated fibroblasts. This effect of JWH015 on IL-6 was completely

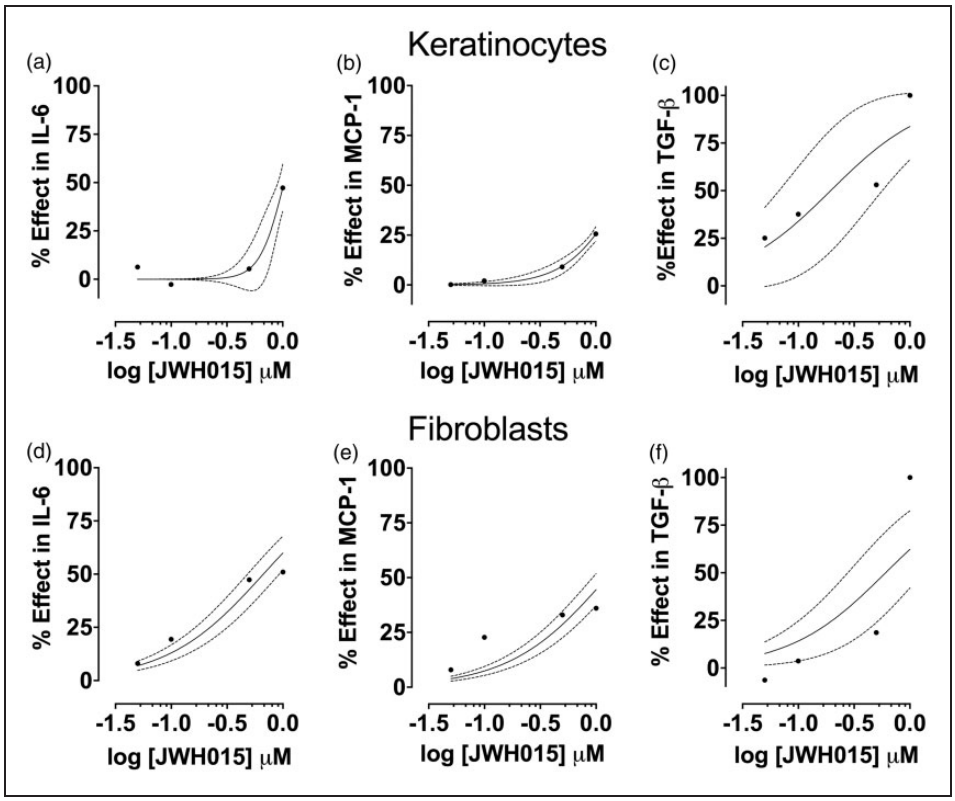

Figure 4. Percent of the effect of JWH015 in cytokines produced by keratinocytes or fibroblasts challenged with LPS. Concentration-response curves for IL-6 (a and d), MCP-1 (b and e) and TGF-β (c and f) in keratinocytes or fibroblasts (respectively) stimulated with LPS (10 and 5 μg/mL, respectively) for 24 h and treated with JWH015. Each bar represents the mean ± SD of 6 samples. LPS: lipopolysaccharide; IL-6: interleukin-6; MCP-1: monocyte chemoattractant protein-1; TGF-β: transforming growth factor-beta.

Table 1. Effective concentration 50 (EC50), percentage of efficacy and minimum effective concentration (MEC) of JWH015 in keratinocytes and fibroblast stimulated with LPS.

	EC50 (μM)		Efficacy (%)		MEC (μM)	
Cytokine	Keratinocytes	Fibroblasts	Keratinocytes	Fibroblasts	Keratinocytes	Fibroblasts
IL-6	1.02 ± 0.01	0.66 ± 0.08	56.67 ± 10.63	58.9 ± 7.61	1	0.5
MPC-1	1.86 ± 0.04	1.24 ± 0.04	31.61 ± 5.99	45.84 ± 3.84	0.5	0.1
TGF-β	0.19 ± 0.17	0.60 ± 0.02	66.56 ± 14.64	54.62 ± 17.15	1	1

Note: For the conditions in which the 50% effect of JWH015 was not completely reached the EC50 was calculated by extrapolation. EC50: effective concentration 50; MEC: minimum effective concentration; IL-6: interleukin-6; MCP-1: monocyte chemoattractant protein-1; TGF-β: transforming growth factor-beta.

blocked by AM630 or AM281 antagonists/inverse agonists (Figure 5(d)). Similarly, the concentration of MCP-1 was significantly decreased by JWH015 when added to LPS-stimulated fibroblasts. This decrease of MCP-1 induced by JWH015 was blocked by either AM630 or AM281 antagonists/inverse agonists (Figure 5(e)). The addition of JWH015 to LPS-stimulated fibroblasts increased the concentration of TGF-β, as previously shown, and this effect was blocked by either AM630 or AM281 antagonists/inverse agonists (Figure 5(f)).

These findings suggest that the effects of JWH015 are mainly mediated by CB1 and CB2 receptors, except for the decrease of MCP-1 in keratinocyte that is predominantly induced via CB2 receptors.

Effects of JWH015 in an in vitro model of wound healing

Given that JWH015 showed a prominent anti-inflammatory effect, and, specifically, induced an increase in TGF-β

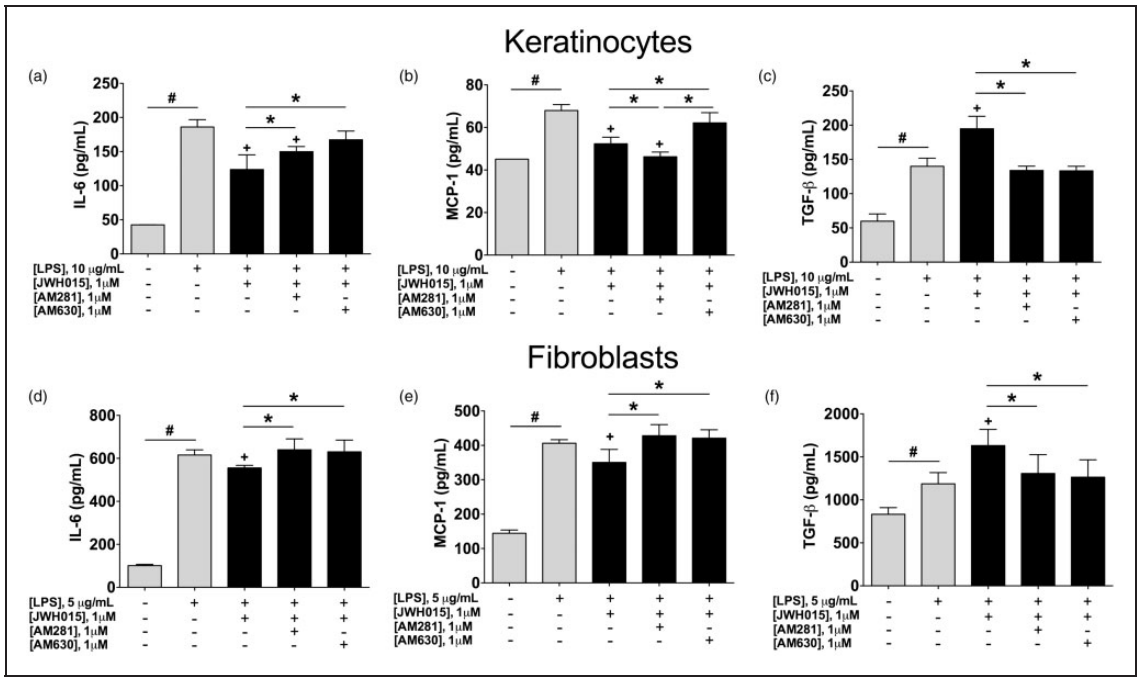

Figure 5. Blockade of JWH015's effects in cytokines produced by keratinocytes or fibroblasts by CB1 or CB2 receptor antagonist/inverse agonist. Concentrations of IL-6 (a and d), MCP-1 (b and e) and TGF-β (c and f) in keratinocytes or fibroblast (respectively) stimulated with LPS (10 and 5 μg/mL, respectively) and concomitantly incubated with 1 μM of JWH015 alone, JWH015 (1 μM) + AM281 (1 μM, CB1 antagonist/inverse agonist) or, JWH015 (1 μM) + AM630 (1 μM, CB2 antagonist/inverse agonist). Each bar represents the mean ± SD of six samples. $^{\#}P < 0.05$ vs. non-stimulated cells, $+P < 0.05$ vs. control group (LPS + vehicle) using One-way ANOVA followed by Dunnett's post hoc test. $^{*}P < 0.05$ between connected groups using One-way ANOVA followed by Tukey's post hoc test. LPS: lipopolysaccharide; IL-6: interleukin-6; MCP-1: monocyte chemoattractant protein-1; TGF-β: transforming growth factor-beta.

(a well-documented pro-wound healing factor), we investigated whether JWH015 plays any role in the scratch assay model (in vitro) of wound healing. The co-culture of fibroblasts and keratinocytes was challenged with 10 μg/mL of LPS and, concomitantly, exposed to the following conditions: LPS + vehicle (0.2% DMSO in PBS), LPS + 1 μM of JWH015 alone, LPS + 1 μM of JWH015 + 1 μM of AM281 (CB1 antagonist/inverse agonist), and LPS + 1 μM of JWH015 + 1 μM of AM630 (CB2 antagonist/inverse agonist). All data were normalized to the control time point for all groups, 0 h, to control for baseline variations and the percent of gap closure was determined. In unpublished data, we have observed that the gap closure of the scratch in keratinocytes and fibroblasts in co-culture is approximately 23–45% at 17 and 19 h (preliminary data).

We observed that the scratch in keratinocytes and fibroblasts in co-culture was 24–27% closed in the LPS + vehicle group at 17- and 24-h time points, respectively. When JWH015 and LPS were simultaneously added to the co-culture, the scratch gap was 36–40% closed at 17- and 24-h time points, respectively (Figure 6). Interestingly, the addition of JWH015 to the co-culture wound produced a faster and more efficient closure of the scratch width when compared with the LPS control group at 12, 17, and 24 h after LPS addition (Figure 7). Either AM281 or AM630 blocked this effect produced by JWH015 at 12, 17, and 24 h after the scratch (Figure 7). These findings suggest that the wound healing effects, as many of the cytokine modulation, induced by JWH015 in the scratch assay model is modulated via CB1 and CB2 receptors.

We determined that the addition of LPS alone (88.3 ± 1.1% of viable cells) or LPS with JWH015 (91.7 ± 2.3% of viable cells) did not produce any significant cytotoxicity in co-cultured keratinocytes and fibroblasts when compared to non-stimulated cells (91.6 ± 1.2% of viable cells).

Transdermal and topical delivery of JWH015 in porcine skin

We determined the ability of JWH015 to reach keratinocytes and fibroblasts when applied to the skin by measuring its topical and transdermal penetration in an ex vivo porcine skin model.

The samples of porcine skin were incubated with 0.5 mL of mineral oil containing 5% JWH015 or

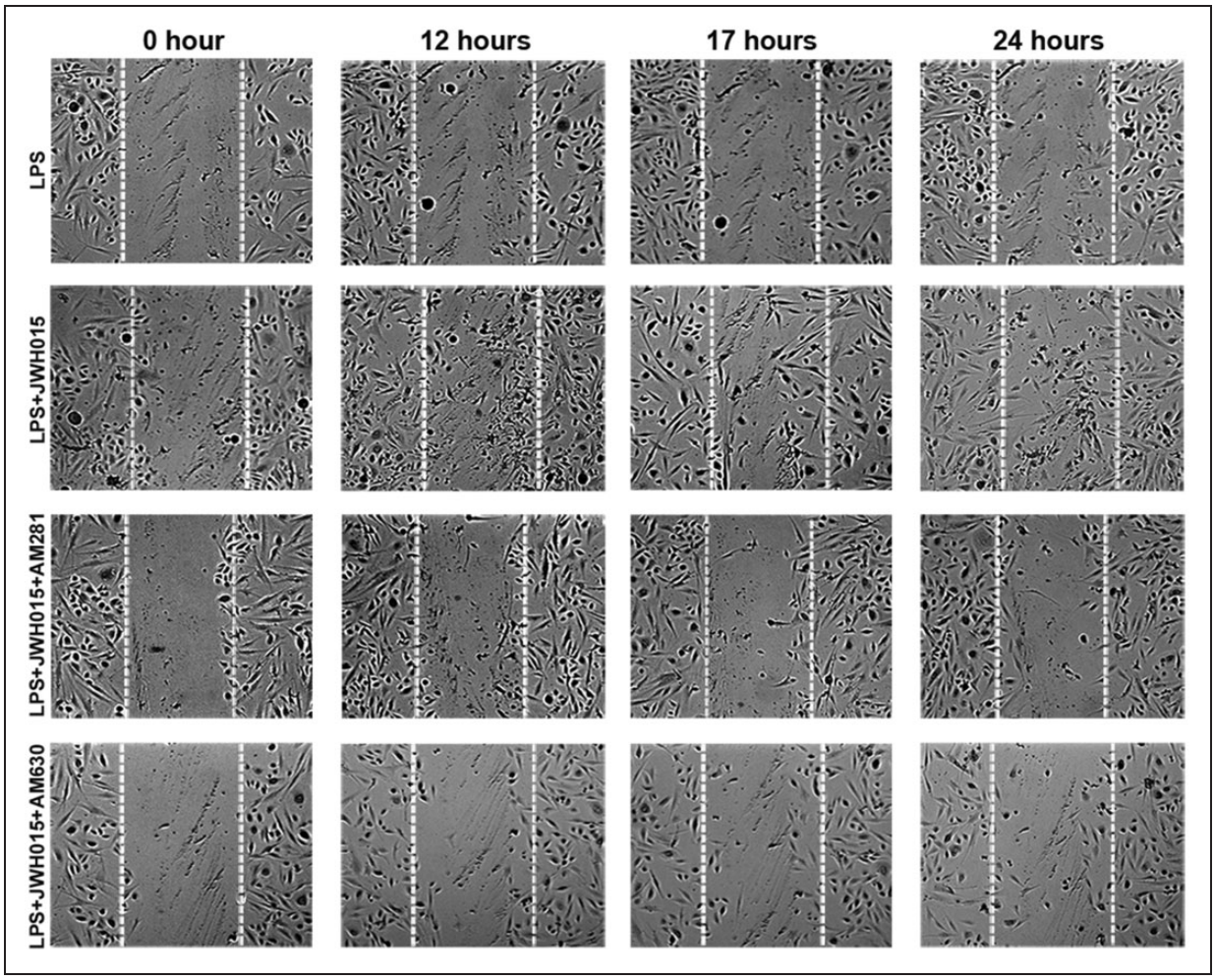

Figure 6. Representative photomicrographs showing the wound closure time course. The scratch assay was performed in LPS-stimulated keratinocytes and fibroblast co-cultures in the presence or the absence of JWH015 (1 μM) with or without a CB1 (AM281, 1 μM) or CB2 (AM630, 1 μM) antagonist/inverse agonist.

0.5 mL control vehicle containing mineral oil only. The samples were taken at 0, 0.5, 1, 2, 3, 4, 5, 6, 12 and 24 h after the addition of the drug. The samples were analyzed by LC-MS to detect the amount of JWH015 that had passed through the skin to reach the receptor compartment. The transdermal concentration (delivery) of JWH015 was only significantly higher at 3 h, the time in which the transdermal concentration of JWH015 peaked in our system (73.62 ± 0.05 ng/cm^2). The transdermal JWH015 concentrations were not significantly different at any other time point tested, and remained lower than 34.92 ± 0.04 ng/cm^2 (Figure 8).

We evaluated the retention of JWH015 in porcine skin 24 h after its topical delivery. High levels of the drug were retained in the skin tissue under our conditions. The average tissue concentration of JWH015 was 881 ± 191 mg/g in the drug-treated tissues, which was significantly higher in comparison to the control (vehicle) group (Figure 9).

Discussion

The major findings of our studies are: (1) The addition of an inflammatory stimulus (i.e. LPS) to primary human keratinocytes and fibroblasts induced an increase in the expression of CB1 and CB2 receptors at the mRNA level; (2) JWH015 reduced the concentration of major pro-inflammatory factors (i.e. IL-6 and MCP-1) and enhanced the concentration of a major anti-inflammatory factor (i.e. TGF-β) in primary human keratinocyte and fibroblast cultures; (3) JWH015 induced a more efficient in vitro wound healing process in primary human keratinocytes and fibroblasts co-cultures; (4) the immunomodulatory and pro-wound healing effects of JWH015 were promoted mostly through both CB1 and CB2 receptors; and (5) JWH015 administered transdermally is mostly retained in the skin and displays a sustained and low transdermal distribution. Our findings offer data that support the use of cannabinoids to

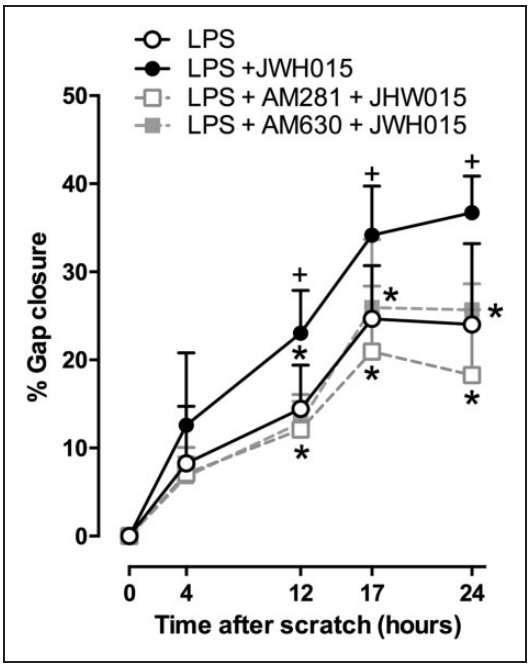

Figure 7. Effect of JWH015 in the in vitro scratch assay. Quantification of gap closure represented as percentage in a wounded (scratch) co-culture of keratinocytes and fibroblast in the presence or the absence of LPS (10 and 5 μg/mL, respectively) and with LPS with 1 μM of JWH015 with or without a CB1 (AM281) or CB2 (AM630) antagonist/inverse agonist. Data shown are means ± SD; $n = 5$–6 samples. + $P < 0.05$ vs. control group (LPS + vehicle), *$P < 0.05$ vs. LPS + JW015 using Two-way ANOVA with repeated measures followed by Tukey's post hoc test. LPS: lipopolysaccharide.

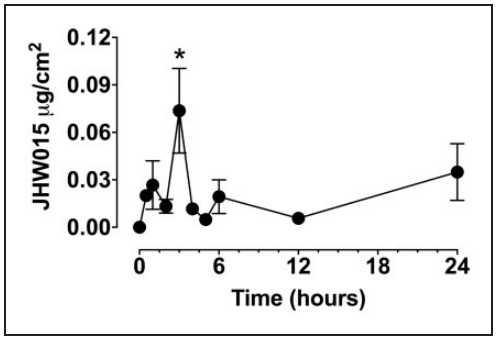

Figure 8. Transdermal delivery of JWH015 in an ex vivo model. Quantification of JWH015 by from samples taken at 0, 0.5, 1, 2, 3, 4, 5, 6, 12 and 24 h after the addition of JWH015 or vehicle on pig skin tissue mounted in Franz cells. Data shown are means ± SD; $n = 5$ samples. *$P < 0.05$ vs. 0 h using One-way ANOVA followed by Dunnett's post hoc test.

target skin cells for the treatment of peripheral inflammatory conditions.

In accordance with previous observations in keratinocytes[43] and fibroblasts,[44] our data indicate that the

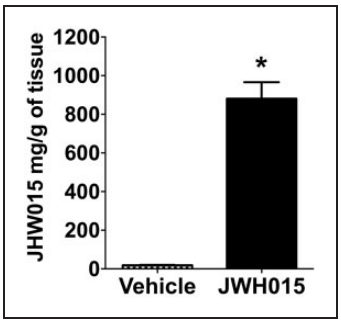

Figure 9. Retention of JWH015 on pig tissue. Quantification of JWH015 in pig skin tissues incubated with JWH015 for 24. Data shown are means ± SD; $n = 3$–6 samples. *$P < 0.05$ vs. vehicle using Student's t-test.

cannabinoid system in skin cells is positively regulated on demand (under pathological conditions), as it has been described in other systems.[13,45,46] Therefore, cannabinoid receptors in keratinocytes and fibroblasts are suitable targets under pathological inflammatory conditions.

The immunomodulatory effects displayed by JWH015 in human keratinocytes and fibroblasts are in line with its effects on cytokine production in other cells of the immune system, such as macrophages,[47] lymphocytes,[48] or microglia.[13] The reduction of IL-6 and IL-8 by cannabinoid receptor activation has been previously shown in human synovial-like fibroblasts stimulated with IL-1β using non-selective cannabinoids.[29] These compounds have been associated in vivo with psychotropic side effects.[49,50] Similarly, anandamide (AEA) decreases MCP-1, IL-6, and IL-8 in LPS-stimulated gingival fibroblasts and those effects are mediated by both CB1 and CB2 receptors.[44] JWH015, which is a relatively low potency preferential CB2 agonist with a K_i of 13.8 nM for CB2 and 383 nM for CB1, has been shown to be effective in reducing pain-related behaviors and modulating inflammatory responses in the spinal cord without inducing psychotropic effects even when administered intrathecally.[18,19] These data together suggest that cannabinoids with relatively low potency (at least through CB1 receptors) are devoid of the central side effects associated with potent cannabinoids; yet, this low potency is sufficient to induce an anti-inflammatory phenotype in skin cells.

All these pro- and anti-inflammatory factors are pivotal in the generation and resolution of inflammation and tissue repair in a variety of inflammatory or painful conditions. Interleukin-6 is quickly detected in response to injury and its increase is correlated with the degree of tissue damage.[51] Increased IL-6 levels have been reported following surgeries and burns and are correlated with the development of postoperative pain.[52–54] Likewise, MCP-1 release is increased in the early stages of tissue repair after injury[55] and exerts its main effects through

the recruitment of cells to the site of the injury.[56] MCP-1 has an important role in early stages of the healing process,[55,57] and it is correlated with pain in patients with temporomandibular disorders[58] and fibromyalgia.[59] Peripheral MCP-1 is important in a mice model of chronic neuropathic pain.[60]

Keratinocytes and fibroblasts are also able to produce pro-wound healing factors, such as TGF-β. This anti-inflammatory molecule mediates the restoration of homeostasis following tissue injury[61,62] and is necessary for proper wound healing.[63] Interestingly, the local administration of recombinant TGF-β into mouse hind paws reduces mechanical hyperalgesia in a murine model of neuropathic pain.[64] Our findings indicate that the increase in TGF-β from skin cells induced by JWH015 could explain at least in part the improved wound healing process observed in our studies. Accordingly, the activation of both CB1 and CB2 receptors has been shown to improve the wound closure in the scratch assay using single cell cultures of human gingival fibroblasts.[65] Furthermore, it seems that the activation of CB2 receptors reduces the fibrotic formation in a wound model in mice through the modulation of TGF-β in late stages of the wound healing process.[66] This anti-fibrotic effect mediated by CB2 receptor activation has been confirmed in CB2 receptor knockout mice studies.[67] On the other hand, CB1 receptors activation promotes a fibrotic response in mice.[68] In fact, it seems that CB1 and CB2 receptors possess opposite effects in some skin cell functions, such as in epidermal permeability in a mouse model.[69]

These data together suggest that the activation of cannabinoid receptors in skin cells may be particularly attractive to modulate the inflammatory process, reduce pain and promote a more efficient tissue repair in post-surgical or post-burn conditions.

JWH015 or other cannabinoids display differential receptor dependence for the modulation of different cellular functions.[13,19,30,47,48] However, it is clear that the effects of JWH015 at concentrations $\leqslant 1\,\mu M$ in human skin cells are anti-inflammatory and non-selective to CB1 or CB2 receptors, while its effects in macrophages, lymphocytes, and the CNS (at least in rodents) seem to be mediated mainly via CB2 receptors. This intriguing feature could represent an advantageous property for this type of compounds since a dual CB1/2 receptor activity could provide a wider spectrum of beneficial effects in skin cells when administered locally, while they will be devoid of CB1-dependent central side effects if they reach systemic and central distribution.

Peripheral administered therapies are getting increasing attention for conditions with predominantly peripheral inflammatory mechanisms, such as psoriasis, arthritis, postoperative pain, burns, etc. Most of the attention has been paid to the modulation of peripheral immune cells. However, there is mounting evidence that demonstrates skin cells could play a prominent role in many states with peripheral inflammation. Since these cells are readily accessible, they represent ideal drug targets, as demonstrated in our topical/transdermal ex vivo system. Whereas hydrophobic and macromolecules are poorly permeable to skin, lipophilic compounds possess a better profile for topical or transdermal delivery. Using our ex vivo system, we determined the high logP of JWH015 to be 5.18, as predicted by ChemDraw Software (Perkin Elmer, Wlatham, MA), confirming the hydrophobic nature of the compound. This is in agreement with the low amount of JWH015 that passed across the flow-through diffusion cell system and the high concentrations of the compound that was retained in the skin. This is in accordance with other drugs with high logP (fentanyl, logP 4.05) that form a depot in skin.[70] In our system, we used porcine skin, which has been extensively used for transdermal delivery studies for other drugs due to the similarities to human skin with regard to lipid composition and subcutaneous fat content.[42,71] It has been shown that intact human skin (stratum corneum) exhibits a certain level of resistance to the diffusion of the cannabinoid delta(9)-tetrahydrocannabinol (delta(9)-THC) in propylene glycol:water:ethanol (9:1:0.4).[72] Our data are in agreement with previous studies which demonstrated that delta(8)-THC possess the same transdermal permeability in human skin and guinea pig skin in vitro.[73] Similarly, it has been shown that both WIN 55212-2 and CP55940 (synthetic cannabinoids) are very permeable through human skin in an in vitro system, in which WIN55212-2 displays a more rapid transdermal diffusion and higher deposition concentration in skin than CP55940.[74] The skin depot effect observed with JWH015 in our studies could be reduced under in vivo conditions due to the presence of the vasculature and blood circulation, and/or by different solvents or vehicles. However, our data indicate that keratinocytes and fibroblasts would be exposed to the drug for relatively long periods of time. This feature is clinically relevant not only for the effects observed in our study but also for the implications in terms of administration frequency and patient compliance in clinical settings.

Conclusions

Selective CB2 receptor agonists have displayed promising results in animal pre-clinical models, however they have yielded disappointing results in small clinical studies (capsaicin-induced pain model and tooth extraction pain). A possible explanation for this lack of translatability from the bench to the bedside is the differential molecular or cellular functions or mechanisms between rodents and humans. The use of human primary skin

cells confers a high translational value to our studies, as suggested in studies that have demonstrated that human and rodent cells respond differently to stimuli and to drugs (i.e. propentofylline, a glial modulator).[18] Together, our data demonstrate that human keratinocytes and fibroblasts are ideal targets to cannabinoids for the treatment of conditions with predominantly peripheral inflammatory or injured tissue pathophysiological mechanisms. Cannabinoid agonists seem to be suitable to target skin cells due to their high lipophilic nature. Direct actions on keratinocytes and fibroblasts through CB1 and CB2 receptors will promote an anti-inflammatory, yet pro-tissue repair phenotype. These effects could also provide beneficial effects in conditions accompanied by pain (burns, postoperative pain, arthritis, war wounds, etc.). Our findings set the foundation for testing this hypothesis using co-cultures with other immune cells such as macrophages and in vivo models of inflammation or tissue injury. This would set the foundation for more informed clinical trials.

Authors' note

AB and PAAV contributed equally to this article. SA and ARS contributed to the design of the experiments. AB, PAAV, CMV, KGV and GG performed the experiments. AB and PAAV analyzed the data. AB, PAAV, ARS, SA contributed to the writing of the manuscript. ARS and SA directed the research.

Declaration of Conflicting Interest

The author(s) declared no potential conflicts of interest with respect to the research, authorship, and/or publication of this article.

Funding

The author(s) disclosed receipt of the following financial support for the research, authorship, and/or publication of this article: This work was supported by IACP grant 2016 (SA). Rita Allen Foundation & American Pain Society 2011 Pain Grant (AR-S); NIH/NIGMS, R15GM109333 (AR-S).

Supplemental Material

Supplementary material for this paper can be found at http://journals.sagepub.com/doi/suppl/10.1177/1744806916688220.

References

1. Amaya F, Izumi Y, Matsuda M, et al. Tissue injury and related mediators of pain exacerbation. *Curr Neuropharmacol* 2013; 11: 592–597.
2. Stockbridge EL, Suzuki S and Pagan JA. Chronic pain and health care spending: an analysis of longitudinal data from the Medical Expenditure Panel Survey. *Health Serv Res* 2015; 50: 847–870.
3. Chan HN, Fam J and Ng BY. Use of antidepressants in the treatment of chronic pain. *Ann Acad Med Singapore* 2009; 38: 974–979.
4. Ryder SA and Stannard CF. Treatment of chronic pain: antidepressant, antiepileptic and antiarrhythmic drugs. *Contin Educ Anaesth Crit Care Pain* 2005; 5: 18–21.
5. Romero-Sandoval EA, McCall C and Eisenach JC. Alpha2-adrenoceptor stimulation transforms immune responses in neuritis and blocks neuritis-induced pain. *J Neurosci* 2005; 25: 8988–8994.
6. Romero-Sandoval A, Bynum T and Eisenach JC. Analgesia induced by perineural clonidine is enhanced in persistent neuritis. *Neuroreport* 2007; 18: 67–71.
7. Ferrari LF, Bogen O, Chu C, et al. Peripheral administration of translation inhibitors reverses increased hyperalgesia in a model of chronic pain in the rat. *J Pain* 2013; 14: 731–738.
8. Campbell CM, Kipnes MS, Stouch BC, et al. Randomized control trial of topical clonidine for treatment of painful diabetic neuropathy. *Pain* 2012; 153: 1815–1823.
9. Kiani J, Sajedi F, Nasrollahi SA, et al. A randomized clinical trial of efficacy and safety of the topical clonidine and capsaicin in the treatment of painful diabetic neuropathy. *J Res Med Sci* 2015; 20: 359–363.
10. Jones VM, Moore KA and Peterson DM. Capsaicin 8% topical patch (Qutenza) – a review of the evidence. *J Pain Palliat Care Pharmacother* 2011; 25: 32–41.
11. Peppin JF and Pappagallo M. Capsaicinoids in the treatment of neuropathic pain: a review. *Ther Adv Neurol Disord* 2014; 7: 22–32.
12. Lynch ME and Ware MA. Cannabinoids for the treatment of chronic non-cancer pain: an updated systematic review of randomized controlled trials. *J Neuroimmune Pharmacol* 2015; 10: 293–301.
13. Romero-Sandoval EA, Horvath R, Landry RP, et al. Cannabinoid receptor type 2 activation induces a microglial anti-inflammatory phenotype and reduces migration via MKP induction and ERK dephosphorylation. *Mol Pain* 2009; 5: 25.
14. Bridges D, Ahmad K and Rice AS. The synthetic cannabinoid WIN55,212-2 attenuates hyperalgesia and allodynia in a rat model of neuropathic pain. *Br J Pharmacol* 2001; 133: 586–594.
15. Munro S, Thomas KL and Abu-Shaar M. Molecular characterization of a peripheral receptor for cannabinoids. *Nature* 1993; 365: 61–65.
16. Herkenham M, Lynn AB, Little MD, et al. Cannabinoid receptor localization in brain. *Proc Natl Acad Sci USA* 1990; 87: 1932–1936.
17. Moreira FA, Grieb M and Lutz B. Central side-effects of therapies based on CB1 cannabinoid receptor agonists and antagonists: focus on anxiety and depression. *Best Pract Res Clin Endocrinol Metab* 2009; 23: 133–144.
18. Landry RP, Martinez E, DeLeo JA, et al. Spinal cannabinoid receptor type 2 agonist reduces mechanical allodynia and induces mitogen-activated protein kinase phosphatases in a rat model of neuropathic pain. *J Pain* 2012; 13: 836–848.
19. Romero-Sandoval A and Eisenach JC. Spinal cannabinoid receptor type 2 activation reduces hypersensitivity and spinal cord glial activation after paw incision. *Anesthesiology* 2007; 106: 787–794.

20. Hansson E and Skioldebrand E. Coupled cell networks are target cells of inflammation, which can spread between different body organs and develop into systemic chronic inflammation. *J Inflamm (Lond)* 2015; 12: 44.
21. Ritter-Jones M, Najjar S and Albers KM. Keratinocytes as modulators of sensory afferent firing. *Pain* 2016; 157: 786–787.
22. Ibrahim MM, Porreca F, Lai J, et al. CB2 cannabinoid receptor activation produces antinociception by stimulating peripheral release of endogenous opioids. *Proc Natl Acad Sci USA* 2005; 102: 3093–3098.
23. Wei T, Guo TZ, Li WW, et al. Keratinocyte expression of inflammatory mediators plays a crucial role in substance P-induced acute and chronic pain. *J Neuroinflammation* 2012; 9: 181.
24. Zhao P, Barr TP, Hou Q, et al. Voltage-gated sodium channel expression in rat and human epidermal keratinocytes: evidence for a role in pain. *Pain* 2008; 139: 90–105.
25. Bartok B and Firestein GS. Fibroblast-like synoviocytes: key effector cells in rheumatoid arthritis. *Immunol Rev* 2010; 233: 233–255.
26. Khamaisi M, Katagiri S, Keenan H, et al. PKCdelta inhibition normalizes the wound-healing capacity of diabetic human fibroblasts. *J Clin Invest* 2016; 126: 837–853.
27. Buckley CD. Why does chronic inflammation persist: an unexpected role for fibroblasts. *Immunol Lett* 2011; 138: 12–14.
28. Buckley CD, Pilling D, Lord JM, et al. Fibroblasts regulate the switch from acute resolving to chronic persistent inflammation. *Trends Immunol* 2001; 22: 199–204.
29. Selvi E, Lorenzini S, Garcia-Gonzalez E, et al. Inhibitory effect of synthetic cannabinoids on cytokine production in rheumatoid fibroblast-like synoviocytes. *Clin Exp Rheumatol* 2008; 26: 574–581.
30. Wilkinson JD and Williamson EM. Cannabinoids inhibit human keratinocyte proliferation through a non-CB1/CB2 mechanism and have a potential therapeutic value in the treatment of psoriasis. *J Dermatol Sci* 2007; 45: 87–92.
31. Karsak M, Gaffal E, Date R, et al. Attenuation of allergic contact dermatitis through the endocannabinoid system. *Science* 2007; 316: 1494–1497.
32. Lebre MC, van der Aar AM, van Baarsen L, et al. Human keratinocytes express functional Toll-like receptor 3, 4, 5, and 9. *J Invest Dermatol* 2007; 127: 331–341.
33. Tardif F, Ross G and Rouabhia M. Gingival and dermal fibroblasts produce interleukin-1 beta converting enzyme and interleukin-1 beta but not interleukin-18 even after stimulation with lipopolysaccharide. *J Cell Physiol* 2004; 198: 125–132.
34. Ndong C, Landry RP, Saha M, et al. Mitogen-activated protein kinase (MAPK) phosphatase-3 (MKP-3) displays a p-JNK-MAPK substrate preference in astrocytes in vitro. *Neurosci Lett* 2014; 575: 13–18.
35. Livak KJ and Schmittgen TD. Analysis of relative gene expression data using real-time quantitative PCR and the 2(-Delta Delta C(T)) Method. *Methods* 2001; 25: 402–408.
36. Walter MN, Wright KT, Fuller HR, et al. Mesenchymal stem cell-conditioned medium accelerates skin wound healing: an in vitro study of fibroblast and keratinocyte scratch assays. *Exp Cell Res* 2010; 316: 1271–1281.
37. Li J, Zheng CQ, Li Y, et al. Hepatocyte growth factor gene-modified mesenchymal stem cells augment sinonasal wound healing. *Stem Cells Dev* 2015; 24: 1817–1830.
38. Liang CC, Park AY and Guan JL. In vitro scratch assay: a convenient and inexpensive method for analysis of cell migration in vitro. *Nat Protoc* 2007; 2: 329–333.
39. Huffman JW and Dai D. Design, synthesis and pharmacology of cannabimimetic indoles. *Bioorg Med Chem Lett* 1994; 4: 360–366.
40. Bell MR, D'Ambra TE, Kumar V, et al. Antinociceptive (aminoalkyl)indoles. *J Med Chem* 1991; 34: 1099–1110.
41. Heustess A, Spigener S, Sweitzer S, et al. Analgesic efficacy and transdermal penetration of topical gabapentin creams: finding an optimal dose and pre-treatment time. *Int J Pharm Compd* 2015; 19: 167–173.
42. Bryson E, Hartman R, Arnold J, et al. Skin permeation and antinociception of compounded topical cyclobenzaprine hydrochloride formulations. *Int J Pharm Compd* 2015; 19: 161–166.
43. Maccarrone M, Di Rienzo M, Battista N, et al. The endocannabinoid system in human keratinocytes. Evidence that anandamide inhibits epidermal differentiation through CB1 receptor-dependent inhibition of protein kinase C, activation protein-1, and transglutaminase. *J Biol Chem* 2003; 278: 33896–33903.
44. Nakajima Y, Furuichi Y, Biswas KK, et al. Endocannabinoid, anandamide in gingival tissue regulates the periodontal inflammation through NF-kappaB pathway inhibition. *FEBS Lett* 2006; 580: 613–619.
45. Piomelli D. The molecular logic of endocannabinoid signalling. *Nat Rev Neurosci* 2003; 4: 873–884.
46. Jean-Gilles L, Braitch M, Latif ML, et al. Effects of pro-inflammatory cytokines on cannabinoid CB1 and CB2 receptors in immune cells. *Acta Physiol (Oxf)* 2015; 214: 63–74.
47. Tolon RM, Nunez E, Pazos MR, et al. The activation of cannabinoid CB2 receptors stimulates in situ and in vitro beta-amyloid removal by human macrophages. *Brain Res* 2009; 1283: 148–154.
48. McKallip RJ, Lombard C, Fisher M, et al. Targeting CB2 cannabinoid receptors as a novel therapy to treat malignant lymphoblastic disease. *Blood* 2002; 100: 627–634.
49. McGregor IS, Issakidis CN and Prior G. Aversive effects of the synthetic cannabinoid CP 55,940 in rats. *Pharmacol Biochem Behav* 1996; 53: 657–664.
50. Shabani M, Divsalar K and Janahmadi M. Destructive effects of prenatal WIN 55212-2 exposure on central nervous system of neonatal rats. *Addict Health* 2012; 4: 9–19.
51. Gebhard F, Pfetsch H, Steinbach G, et al. Is interleukin 6 an early marker of injury severity following major trauma in humans? *Arch Surg* 2000; 135: 291–295.
52. Summer GJ, Romero-Sandoval EA, Bogen O, et al. Proinflammatory cytokines mediating burn-injury pain. *Pain* 2008; 135: 98–107.
53. Rettig TC, Verwijmeren L, Dijkstra IM, et al. Postoperative interleukin-6 level and early detection of complications after elective major abdominal surgery. *Ann Surg* 2016; 263: 1207–1212.

54. Koch A, Zacharowski K, Boehm O, et al. Nitric oxide and pro-inflammatory cytokines correlate with pain intensity in chronic pain patients. *Inflamm Res* 2007; 56: 32–37.
55. Low QE, Drugea IA, Duffner LA, et al. Wound healing in MIP-1alpha(-/-) and MCP-1(-/-) mice. *Am J Pathol* 2001; 159: 457–463.
56. Ding J and Tredget EE. The role of chemokines in fibrotic wound healing. *Adv Wound Care (New Rochelle)* 2015; 4: 673–686.
57. Wood S, Jayaraman V, Huelsmann EJ, et al. Pro-inflammatory chemokine CCL2 (MCP-1) promotes healing in diabetic wounds by restoring the macrophage response. *PLoS One* 2014; 9: e91574.
58. Slade GD, Conrad MS, Diatchenko L, et al. Cytokine biomarkers and chronic pain: association of genes, transcription, and circulating proteins with temporomandibular disorders and widespread palpation tenderness. *Pain* 2011; 152: 2802–2812.
59. Ang DC, Moore MN, Hilligoss J, et al. MCP-1 and IL-8 as pain biomarkers in fibromyalgia: a pilot study. *Pain Med* 2011; 12: 1154–1161.
60. Zhang H, Boyette-Davis JA, Kosturakis AK, et al. Induction of monocyte chemoattractant protein-1 (MCP-1) and its receptor CCR2 in primary sensory neurons contributes to paclitaxel-induced peripheral neuropathy. *J Pain* 2013; 14: 1031–1044.
61. Elliott CG, Forbes TL, Leask A, et al. Inflammatory microenvironment and tumor necrosis factor alpha as modulators of periostin and CCN2 expression in human non-healing skin wounds and dermal fibroblasts. *Matrix Biol* 2015; 43: 71–84.
62. Woodley DT, Wysong A, DeClerck B, et al. Keratinocyte migration and a hypothetical new role for extracellular heat shock protein 90 alpha in orchestrating skin wound healing. *Adv Wound Care (New Rochelle)* 2015; 4: 203–212.
63. Maarof M, Law JX, Chowdhury SR, et al. Secretion of wound healing mediators by single and bi-layer skin substitutes. *Cytotechnology* 2016; 68: 1873–1884.
64. Lantero A, Tramullas M, Pilar-Cuellar F, et al. TGF-beta and opioid receptor signaling crosstalk results in improvement of endogenous and exogenous opioid analgesia under pathological pain conditions. *J Neurosci* 2014; 34: 5385–5395.
65. Kozono S, Matsuyama T, Biwasa KK, et al. Involvement of the endocannabinoid system in periodontal healing. *Biochem Biophys Res Commun* 2010; 394: 928–933.
66. Li SS, Wang LL, Liu M, et al. Cannabinoid CB2 receptors are involved in the regulation of fibrogenesis during skin wound repair in mice. *Mol Med Rep* 2016; 13: 3441–3450.
67. Akhmetshina A, Dees C, Busch N, et al. The cannabinoid receptor CB2 exerts antifibrotic effects in experimental dermal fibrosis. *Arthritis Rheum* 2009; 60: 1129–1136.
68. Marquart S, Zerr P, Akhmetshina A, et al. Inactivation of the cannabinoid receptor CB1 prevents leukocyte infiltration and experimental fibrosis. *Arthritis Rheum* 2010; 62: 3467–3476.
69. Roelandt T, Heughebaert C, Bredif S, et al. Cannabinoid receptors 1 and 2 oppositely regulate epidermal permeability barrier status and differentiation. *Exp Dermatol* 2012; 21: 688–693.
70. Calis KA, Kohler DR and Corso DM. Transdermally administered fentanyl for pain management. *Clin Pharm* 1992; 11: 22–36.
71. Heustess A, Asbill S, Eagerton D, et al. In vitro skin penetration and skin content of progesterone from various topical formulations. *Int J Pharm Compd* 2014; 18: 512–515.
72. Challapalli PV and Stinchcomb AL. In vitro experiment optimization for measuring tetrahydrocannabinol skin permeation. *Int J Pharm* 2002; 241: 329–339.
73. Valiveti S, Hammell DC, Earles DC, et al. In vitro/in vivo correlation studies for transdermal delta 8-THC development. *J Pharm Sci* 2004; 93: 1154–1164.
74. Valiveti S, Kiptoo PK, Hammell DC, et al. Transdermal permeation of WIN 55,212-2 and CP 55,940 in human skin in vitro. *Int J Pharm* 2004; 278: 173–180.